Arabian Journal for Science and Engineering (2020) 45:8199–8217
https://doi.org/10.1007/s13369-020-04669-2

RESEARCH ARTICLE-CIVIL ENGINEERING

Ternary Diagrams for Predicting Strength of Soil Ameliorated with Different Types of Fly Ash

Adil Binal[1] · **Banu Ebru Binal**[2]

Received: 8 December 2019 / Accepted: 25 May 2020 / Published online: 6 June 2020

Abstract
In recent years, the use of geopolymer materials for ground improvement has increased with the growth in the construction sector. The lignite coal used in the thermal power plants in Turkey has low-calorie content. Thus, fly ash from these thermal power plants has high-lime content, making it unsuitable for cement production or as a cement additive material. Therefore, it is necessary to find different areas where fly ash can be utilised. In this study, the fly ashes of six power plants were tested to improve the properties of cohesive soil. The effects of fly ash along with the soil properties on improving the physicomechanical properties of the soil were examined with different mix designs. The effects of the curing period on the soil strength values were examined, and the unconfined compressive strength values of all mixtures were compared with those of the controlled specimens prepared with optimum water content. In the literature, seventeen various case studies on fly ash–soil remediation have been investigated. The data of this study and other studies were evaluated together, and multiple regression and artificial neural network analyses were performed to estimate the improved soil strength. Additionally, ternary contour diagrams were designed for assessing the fly ash–mixed soil strength using the physical and mechanical properties of the soil and fly ash.

Keywords Fly ash · Geopolymer · Clay · Sand · Ternary diagram

1 Introduction

Swelling in sub-grade soils is a significant problem because it causes surface cracks, heaves, and road foundation failure. One straightforward and conventional method is to remove the soft soil and replace it with gravel and crushed rocks. However, this process is not an economical method for eliminating swelling soils. Therefore, many stabilisation techniques have been developed to prevent the harmful swelling soil effects beneath the structures. One such economical solution is the amelioration of on-site soil with additive materials, such as lime, fly ash, cement, and polymer. Using fly ash to improve soils has a dual benefit: one is that it is the most economical process, and the other is that it eliminates the harmful power plant products without causing any environmental issues. Annually, more than 600 million tons of fly ash is produced worldwide. Thermal power plants in Turkey use approximately 55 million tons of lignite coal each year, and as a result, 16 million tons of fly ash is left to the natural environment as waste [1].

Further, the total amount of fly ash in landfills, ponds, and dams has reached approximately 100 million tons [2]. These figures increase daily worldwide (including Turkey) due to continually increasing energy demands. Moreover, the fly ash generated in Turkey exhibits high alkaline content because of the low-calorie lignite coal burned in thermal power plants. This makes fly ash unsuitable for concrete mix or cement production; thus, fly ash consumption has only reached 2%. Consequently, the introduction of new techniques and approaches that consume fly ash is of significant importance for Turkey and the world.

A pozzolanic material containing a source of silica and alumina that is readily dissolved in solution acts as a source of geopolymer precursor species and lends itself to polymerisation [3–5]. Furthermore, fly ash particles can provide a sufficient range of divalent and trivalent cations under

✉ Adil Binal
adil@hacettepe.edu.tr

[1] Faculty of Engineering, Department of Geological Engineering, Hacettepe University, Beytepe Campus, 06800 Ankara, Turkey

[2] General Directorate of Mineral Research and Explorations, Ankara, Turkey

ionised conditions promoting lumpiness in the dispersed clay. However, bituminous coals have low concentrations of calcium compounds, and the resulting Class "F" fly ash product exhibits no self-cementing characteristics [6]. Subbituminous coals have higher calcium carbonate ($CaCO_3$) levels; therefore, the Class "C" fly ash produced during their combustion is rich in calcium, resulting in self-cementing characteristics. Since Class "C" fly ash is self-cementing, activators such as lime or Portland cement are not required. Upon exposure to water, the Class "C" fly ash hydrates form cementitious products similar to those produced during the hydration of Portland cement. This property makes self-cementing fly ash a very efficient and economic stabilisation agent for use in various construction applications [7]. Few studies on fly ash and soil performance have alleged that Class "C" fly ash improves the physicomechanical properties of the mixed soils [7–12]. Fly ash is used to stabilise fine-grained soils so that a stable working platform can be provided for highway construction equipment [8, 13–15]. Additives with calcium oxide produce flocculation in the clay layers by the substitution of monovalent ions by Ca^{2+} ions. This balances the clay layers electrostatic charge and reduces the electrochemical repulsion forces between them. The clay particle adhesion into flocks occurs, giving rise to soil with improved engineering properties: a more granular structure, less plasticity, higher permeability, and above all, lower expansion [7, 16–20].

The strength and stiffness enhancement of the fly ash–soil mixture can be categorised into two groups, short-term and long-term strength gain. The short-term strength gain of fly ash–soil mixture is usually attributed to the cation exchange process. When fly ash is added to the soil, fly ash particles react with moisture and start hydration. Due to hydration, large amounts of minerals, such as lime (CaO), anhydrite ($CaSO_4$), periclase (MgO), quartz, and tricalcium aluminate, are dissolved; thus, the solution conductivity gradually increases [21]. Further, the presence of the OH^- ions produces an increase in the soil pH up to approximately twelve. Under these conditions, pozzolanic reactions occur when they form a part of the Si and Al clusters and lead to cementing compounds, such as combined Ca^{2+}, calcium silicate hydrates, and calcium aluminate hydrates [7, 19, 20, 22]. The long-term strength of the stabilised soil is associated with curing time. The strength gain is attributed to the pozzolanic reactions. Generally, the pozzolanic reaction is slow and is slowed even further by the formation of a shell of calcium silicate hydrate (CSH) gel around the fly ash particles [21].

Fly ash cenospheres (FACs) are hollow alumino-silicate spheres created as residue from the coal-fired power plants. Due to their hollow nature, the particle density typically ranges from 600 to 900 kg/m^3 [23, 24], making them suitable for producing lightweight composites [24]. However, this is not the only reason for explaining the usage of fly ash in concrete production as well as a soil-stabilising agent. The other reason for the preference of the fly ash is its cation exchange capacity (CEC). The divalent and trivalent cations of fly ash can promote clay particle flocculation [25].

Although many studies have been conducted on soil improvement with fly ash, this research area still has practicality. Recent surveys have been on the prediction strength of the soil mixed with fly ash and cure period effects on physicomechanical properties because the behaviour of the sub-grade soil over long periods is significant for road stabilisation and surface crack formation. In this study, the effects of fly ash additives, varying from 5 to 25%, on the physicomechanical properties of Yenikent/Ankara clay samples were determined by laboratory tests. Furthermore, to estimate the cured and one-day cured compressive strength of the soil mixed with fly ash, new ternary charts were designed using the test data of this study together with those of seventeen different case studies on soil stabilisation. The artificial neural network (ANN) method was used to determine missing data necessary for ternary chart development. The variables of ternary diagrams are fly ash content, liquid limit (LL), plastic limit (PL), clay activity (A_c), optimum water content (OMC), and maximum dry unit weight (MDD) of fly ashes.

2 Materials

In this study, a soil sample collected from the district of Ankara as well as six types of fly ash obtained from Yatağan (YFA), Çatalağzı (CFA), Seyitömer (SeFA), Orhaneli (OFA), Soma (SFA), and Tunçbilek (TFA) was used in the tests (Table 1).

2.1 Soil

For this study, the soil was taken from a construction site located at the Yenikent vicinity of Ankara city (Fig. 1). The sampling depths of the soil blocks were about three metres. The soil colour in the sampling area was light brown and grey. As to sieve analyses, it consists of 54% clay, 24% silt, 7.4% sand, and 14.6% gravel-sized materials. Regarding index properties, it has a PL of 26.1%, LL of 83.1%, and

Table 1 Power plants generating fly ashes used in tests

Power plants	City of Turkey
Yatağan	Denizli
Çatalağzı	Zonguldak
Seyitömer	Kütahya
Orhaneli	Bursa
Soma	Manisa
Tunçbilek	Kütahya

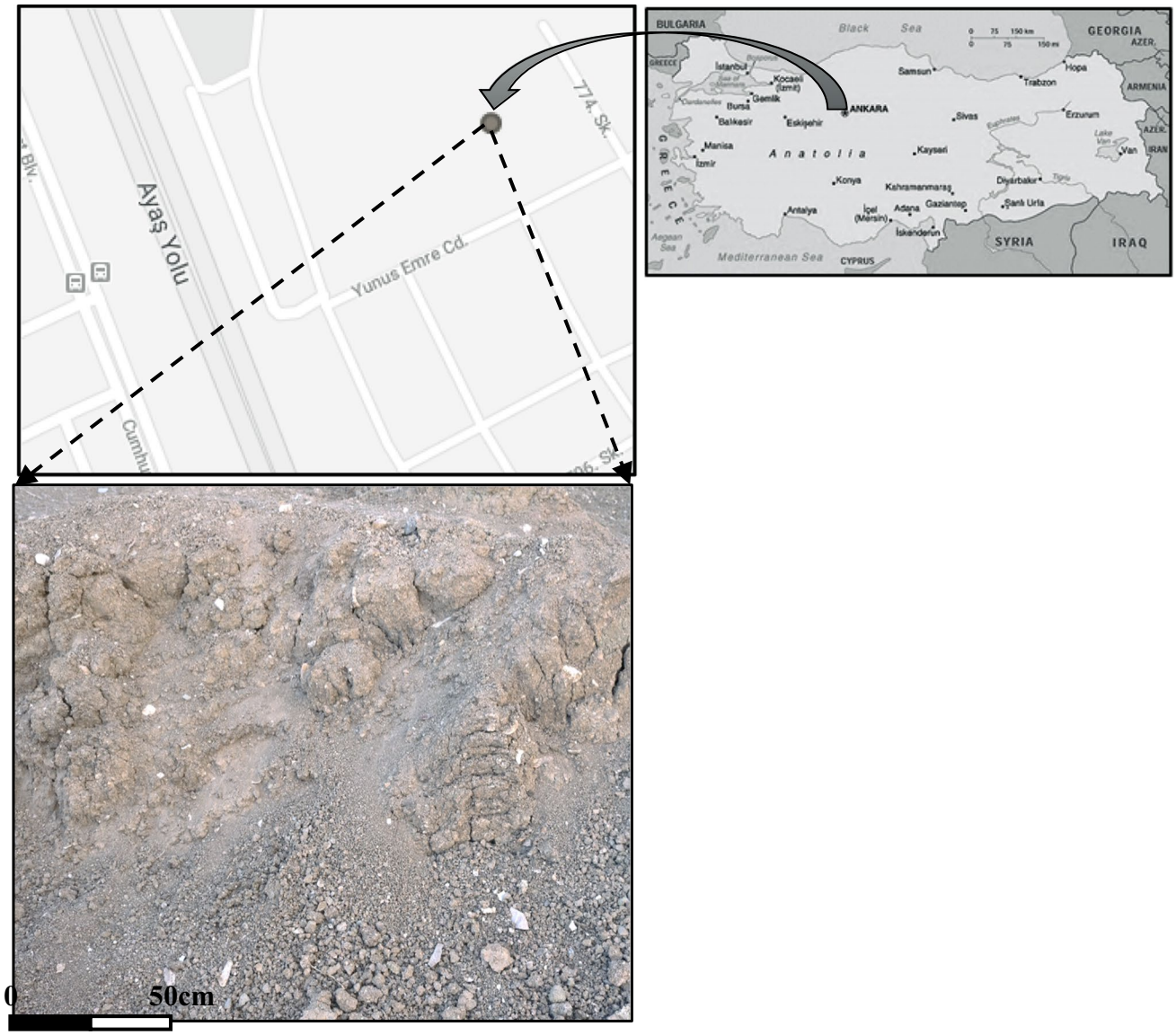

Fig. 1 Sampling area, white grains are the lime lens in the picture

plasticity index (PI) of 57%. The soil sample was identified as "CH" by the unified soil classification system, and its activity is 0.95. Chemical analysis showed that its principal constituents are silica, aluminium, calcium, and iron oxides. The SiO_2, Al_2O_3, and Fe_2O_3 content of the soil sample is 55.36%, 15.59%, and 7.41%, respectively (Table 2). Furthermore, the lime lens formation in the soil (Fig. 1) is the cause of the high calcium content (CaO: 13.27%).

2.2 Fly Ashes

The grain sizes of the fly ashes ranged from 0.002 to 0.2 mm (Fig. 2), and all types of fly ashes were classified as fine-grained materials.

The CECs of these fly ashes were ranked from 1 to 17.44, and their specific surface areas ranged from 0.094 to 0.334 m^2/g (Table 3). The silica content ranged from 25.68 to 47.09%, and the calcium content ranged from 2.82 to 48.15%.

Table 2 Some properties of soil

Clay soil			
Physicomechanical properties		Chemical composition	
G_s	2.60	SiO_2 (%)	55.36
LL (%)	83.1	Al_2O_3 (%)	15.59
PL (%)	26.1	Fe_2O_3 (%)	7.41
PI (%)	57	S + A + F (%)	65.5
A_c	0.95	CaO (%)	13.27
Clay (%)	54	MgO (%)	4.15
Silt (%)	24	SO_3 (%)	0
Sand (%)	7.4	K_2O (%)	2.36
Gravel (%)	14.6	Na_2O (%)	1.86
Finer than no. 200 (%)	78		
σ_u (kPa)	103		

G_s specific gravity, *LL* liquid limit, *PL* plastic limit, *PI* plasticity index, A_c clay activity, c cohesion, ϕ internal friction angle, and σ_u unconfined compressive strength

The SAF ($SiO_2 + Al_2O_3 + Fe_2O_3$) contents in YFA vary from 39.40 to 84.86%. Moreover, SFA was classified as Class C fly ash. CFA and TFA have properties of Class F fly ash. Others do not fulfil the requirements of the ASTM C 618 standard [26].

3 Methods

Laboratory tests were conducted to determine the physicomechanical properties of the soil samples containing 5–25% fly ash, which are to be used as variable parameters in the ternary diagrams. The samples were prepared by the rules of ASTM D7721 and ASTM D698 [28, 29]. In these standards, the soil at a selected moulding water content is placed in three layers into a mould (101.6 mm in diameter), with each layer compacted by 25 blows of a 2.5-kg hammer dropped from a distance of 30 cm. The resulting dry unit weight is determined. The procedure is repeated for an adequate number of moulding water contents to establish a relationship between the dry unit weight and the moulding water content for the soil. The compaction curve is plotted with the dry unit weight and water content values. The amounts of the highest dry unit weight and optimum moisture content are found from the compaction curve. After the OMC determination process, a premeasured quantity of fly ash has been mixed with dry soil and water (at an optimum value) thoroughly to produce a homogeneous fly ash–soil mixture.

Curing periods are more effective on the strength of fly ash–soil mix. In several studies, 14 and 28 days were selected as curing periods [12, 28, 30–36]. Therefore, 28 days was preferred as the curing period in this study. The samples were covered with a stretch film after removal from the moulds to avoid moisture loss and were subsequently placed in a humidity room with a temperature of 21 °C and a relative humidity of 80% for a total of 28 days. Additionally, the one-day cured samples were held in their moulds for 1 day.

The Atterberg limits of the mixed soil samples were tested by ASTM D4318 [37], and the PI values were calculated. The unconfined compressive strengths of the one-day and 28-day cured fly ash–mixed soil samples were tested by ASTM D2166 [38]. The changes in the OMC and MDD values with the addition of fly ash to the examples were investigated.

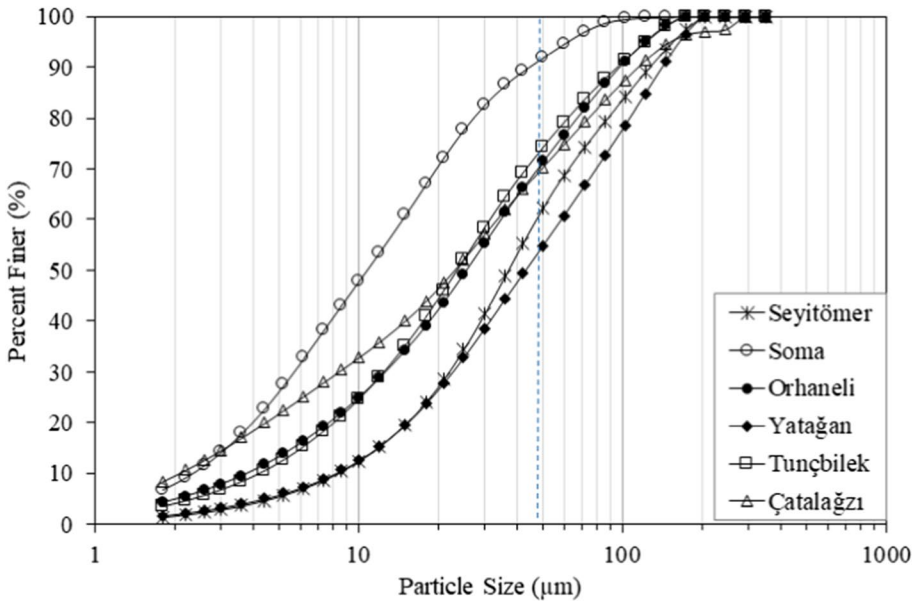

Fig. 2 Grain size distributions of fly ashes tested (The 0.045-mm border is shown by the dashed blue line)

Table 3 Some properties of the fly ashes used in this test

Physicomechanical properties	YFA	CFA	SeFA	OFA	SFA	TFA	ASTM C618 limits (Class C)	ASTM C618 limits (Class F)
G_s	2.35	2.1	2.1	2.4	1.98	1.97		
SSA (m^2/g)	0.334	0.139	0.115	0.303	0.207	0.094		
*CEC	2.61	1	2.21	5.01	17.44	1.4		
Finer than no.200 (%)	67.72	80.27	75.39	83.02	98.09	84.6		
Retained on 0.045 mm(%)	45.1	29.63	37.69	28.5	8.09	25.76	< 34	< 34
SiO_2	37.19	44.66	44.12	25.68	33.33	47.09		
Al_2O_3	24.79	30.56	21.01	5.78	19.61	22.42		
Fe_2O_3	9.92	9.64	15.76	8.03	6.47	15.25		
$SiO_2 + Al_2O_3 + Fe_2O_3$	71.90	84.86	80.88	39.49	59.41	84.75	> 50	> 70
Na_2O	0.62	0.71	1.47	0.16	0.39	0.67		
K_2O	4.75	8.23	3.78	0.64	2.16	3.59		
MgO	3.10	3.29	5.88	5.78	1.76	6.73		
CaO	18.39	2.82	7.35	48.15	35.29	3.81		
SO_3	1.24	0.09	0.63	5.78	0.98	0.45	< 5.0	< 5.0
LOI	1.1	1.12	3.05	1.7	2.7	2.1	< 6.0	< 6.0

YFA Yatağan, *CFA* Çatalağzı, *SeFA* Seyitömer, *OFA* Orhaneli, *SFA* Soma, *TFA* Tunçbilek, G_s specific gravity, *SSA* specific surface area, *CEC* cation exchange capacity, *LOI* loss on ignition

*CEC values obtained from the project of TUBITAK [27]

Other studies based on stabilisation of soil using fly ash and including the same variables as this study were examined to improve the ANN dataset. Data from seventeen case studies including test results of Atterberg limit tests, A_c, OMC, MDD, and unconfined compression strength were collected from articles and together with data of this study were used as input parameters for ANN analysis (Table 4).

4 Laboratory Test Results

The Atterberg limit tests were performed in the laboratory studies. Their PL values increase while LL values decrease with the fly ash addition (Fig. 3a, b). Consequently, the soil begins to exhibit plastic behaviour and low LL depending on the fly ash content. Furthermore, the PI values of the samples decreased from 57 to 32.6%. Therefore, the performance comparison among the spectrum of mixed soils approaches that of sandy soils.

The A_c value of the Yenikent clay decreases with the amount of added fly ash (Fig. 4). This is another observation that shows an increase in the soil plasticity behaviour by the fly ash addition.

As the amount of fly ash increases, the OMC increases and MDD values decrease (Fig. 5). This state may be attributed to the fact that the fly ash has a water holding capacity and low unit weight. The OMC value increases as the amount of fly ash used in the mix is increased (Fig. 5a). The ionic concentration had more effect when the fly ash concentration was low; however, when the fly ash content was high, the sedimentation behaviour was governed more by the fly ash particles than by the ionic concentration. An increase in the percentage of fly ash could cause an increase in the settling speed of fly ash kaolinite soil mixtures [47].

Furthermore, fly ash hydration increased the ionic strength, which changed the kaolinite from dispersed free settling to flocculated zone settling. Fly ash particles were found to collide with the kaolinite particles during settling and form large agglomerates; therefore, the settling rate of fly ash–soil mixture increased with the addition of fly ash [48]. Consequently, the diffuse double-layer (DDL) thickness decreases with fly ash use and causes flocculation of clay particles. This flocculation generates a resistance against the compaction effort, causing an MDD reduction (Fig. 5b).

Further, fly ash particles behave as a binding material between soil particles (especially silt and sand grain size) and improve soil resistance. In this study, the increase in the uniaxial compressive strength (UCS) values of the soil samples was found to be due to the increased fly ash addition (Fig. 6). The curing time also affects the strength of the soil samples with fly ash. With time, fly ash shows increase binding capacity between soil particles, thereby increasing the soil strength.

The changes in the physicomechanical properties of the 25% fly ash samples are presented in Table 5. The highest increase in PL values was seen in the OFA samples. The most considerable change in all other physical properties

Table 4 Dataset of ANN analysis

Fly ash (%)	Power plant	LL (%)	PL (%)	PI (%)	A_c	OMC (%)	MDD kN/m^3	UCS1 (kPa)	UCS28 (kPa)	References
0–25	Yatagan/Turkey	*83.1–68.3	26.1–32.0	57–36.3	0.95–1.49	18.5–24.2	15.3–12.8	103–478	106–625.4	In this study
0–25	Catalagzi/Turkey	83.1–54.2	26.1–30.6	57–23.6	0.95–2.29	18.5–22.0	15.3–11.7	103–468	106–750.2	In this study
0–25	Seyitömer/Turkey	83.1–68.3	26.1–30.1	57–38.2	0.95–1.42	18.5–22.5	15.3–12.8	103–461	106–793.0	In this study
0–25	Orhaneli/Turkey	83.1–92.7	26.1–50.8	57–41.9	0.95–1.29	18.5–15.1	15.3–14.6	103–423	106–638.96	In this study
0–25	Soma/Turkey	83.1–51.9	26.1–35.5	57–16.4	0.95–3.29	18.5–27.9	15.3–11.6	103–666.8	106–1052.4	In this study
0–25	Tunçbilek/Turkey	83.1–75.0	26.1–35.5	57–39.0	0.95–1.38	18.5–21.8	15.3–14.4	103–426	106–478.07	In this study
0–25	Yenikoy/Turkey	*88.7–64.6	35–55.9	53.8–8.8	0.18–1.12	30–34.8	17.9-14.2	27.8–310	27.82–441	[7]
0–25	Montour/USA	*36–45	22–31	10–20.7	0.13–0.22	16–26	13.2–15.6	298–610	390–780	[34]
0–35	Lippendorf/Germany	*50–88.65	28.57–60.4	13.5–34.9	0.15–0.78	23.8–32.7	12.2–14.7	40.9–765.8	25.3–1997.5	[30]
3–10	Tuncbilek/Turkey	*49–50	20.5–21	28–29	0.78–0.81	21.5–23.0	15.4–15.6	11.60–23.8	21.5–26.2	[33]
0–30	Raichur/India					17.8–16.1	15.1–18.2	338.5–550.3	458.1–671.0	[35]
0–20	Soma/Turkey					22–24	14.5–13.6		622–1259	[31]
0–15	Kangal/Turkey	*81.95–89.74	26.55–49.91	55.40–39.82	0.95–0.68	35.8–40.9	13–12.1	176.6–476.1	205.0–1048.1	[12]
0-100	Ackerman/USA					14.0–45.5	17.9–10.4		200–2665	[28]
0–15	AES/Puerto Rico	*68–80	30–35	36–45	0.62–0.78			28–273.9	289.9–489.8	[32]
0–100	India	*228–38	63.4–22	164.6–16	2.11–0.21	26.9–41	12.2–12.7	35.3–381.6		[39]
0–40	Neyveli/India	*53–46	29–25	24–21		31.2–25.2	12.1–15.3	167–218		[40]
0–90	Rourkela/India	*170–40	50–15	120–25	1.79–0.37	26–16	13.7–14.2	42–122.5		[41]
0–40	Ennore/India	*28–30	18–21	8–12	0.13–0.20	18.5–15.4	18.0–15.1	269.7–117.6		[42]
0–10	Soma/Turkey	*23–29	11–14	12–15	0.26–0.33	7.6–8.3	21.5–20.6	47–6	47–642	[43]
0–25		*34.8–32.9	20.2–22.1	13.3–9.2	1.79–0.81	17.8–20.5	17.4–20.01	24.7–45.1		[44]
0–10		*72.1–61	31.7–46.3	40.4–14.7	0.64–0.23	32.5–32	13.4–13.7	312.0–371.5	312.0–405	[45]
0–15		*59.8–52.4	27.5–35.07	32.2–17.3	0.58–0.36	20.8–19.4	16.7–16.4	450.4–570		[46]

UCS1 unconfined compressive strength of the one-day cured sample, *UCS28* unconfined compressive strength of the 28-day cured sample

*First values of the physicomechanical properties are the soil properties used in the studies

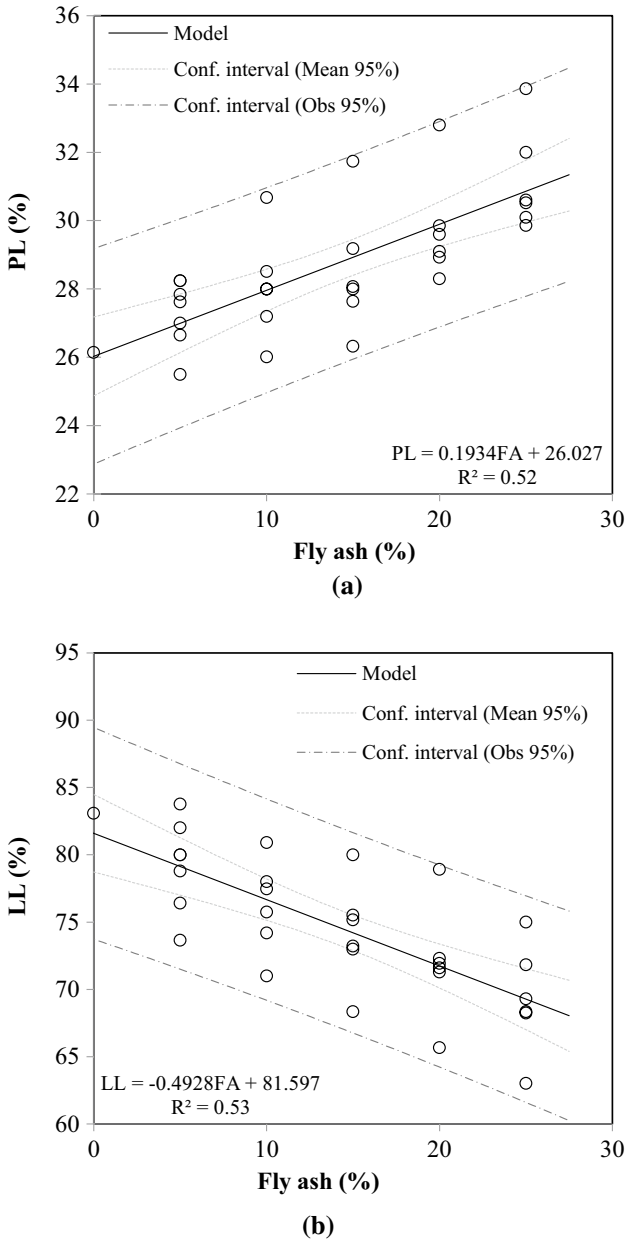

Fig. 3 Atterberg limits of soil samples mixed with the fly ashes from six power plants, **a** for the plastic limit (PL), **b** for the liquid limit (LL)

was observed in the SFA mixture. The soil samples containing 25% SFA increased 547.4% in unconfined compressive strength values and 892.8% in the 28-day cured specimens.

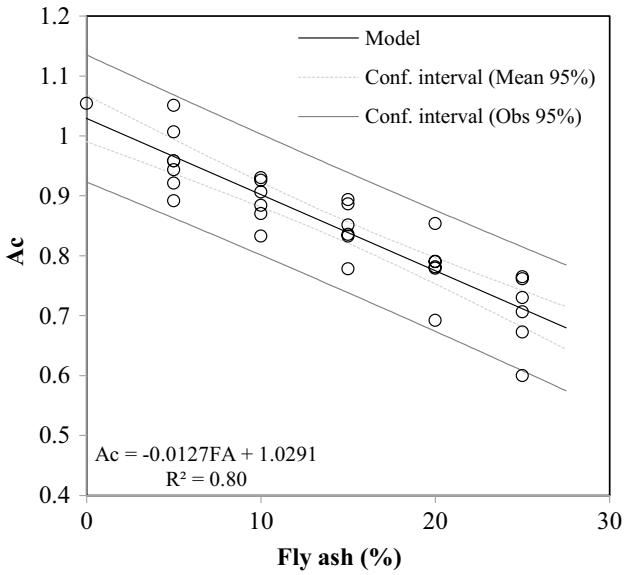

Fig. 4 A_c of samples mixed with the fly ashes

5 Multiple Linear Regression

Regression analysis involves multiple regressor variable states in many applications. The regression model that includes more than one regressor variable is called a multiple linear regression (MLR) model [49] and is represented in Eq. 1:

$$y = \beta_0 + \beta_1 x_{i1} + \cdots + \beta_k x_k + \varepsilon \quad (1)$$

The MLR analyses were performed using the soil physical property data determined in this study and of seventeen other studies in the literature. The statistical evaluation of the variables used in the MLR analyses is presented in Table 6. The fly ash values vary from 0 to 100%. The least standard deviation, as well as coefficient of variance, was shown by the MDD values. The highest ratio of variation belongs to the A_c values. However, the highest difference was observed in the UCS28 data. The UCS of the one-day cured samples ranges from 25 to 410 kPa, and the values of the cured samples varied between 27.8 and 622.3 kPa.

The model equations, composed of all variables used for predicting the one-day and 28-day cured examples, are given in Table 7. The UCS values of the one-day cured soil samples were used in the analyses to estimate the strength values of the soil samples cured for 28 days.

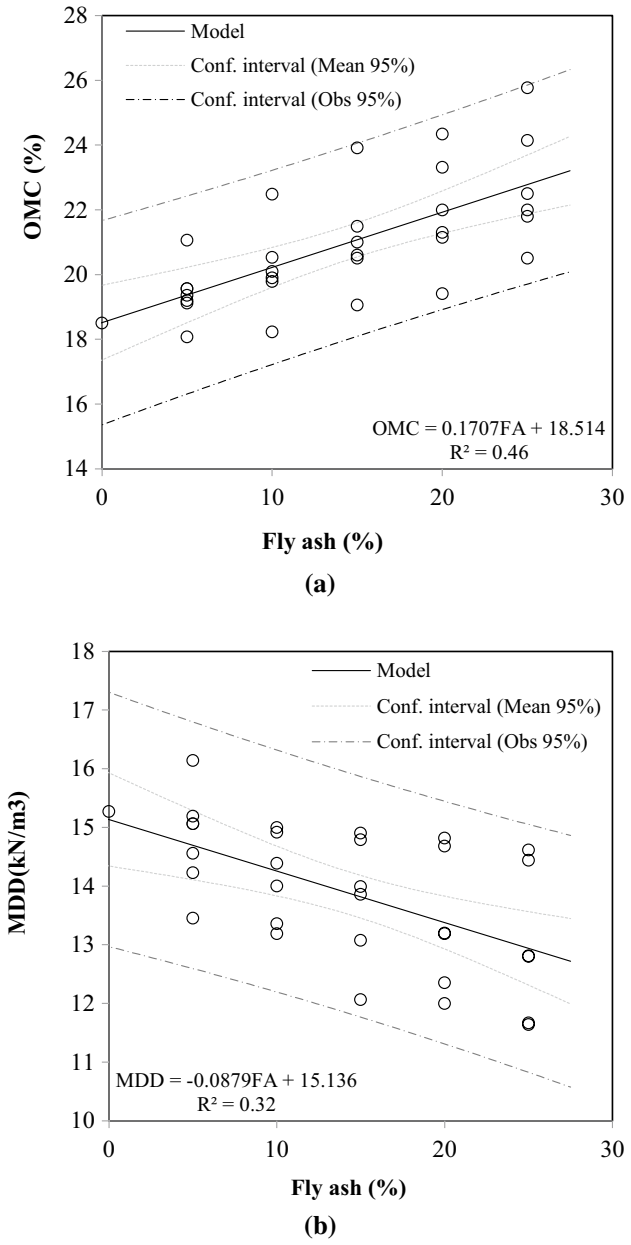

Fig. 5 **a** OMC and **b** MDD results of standard proctor tests of soils including six power plants' fly ashes

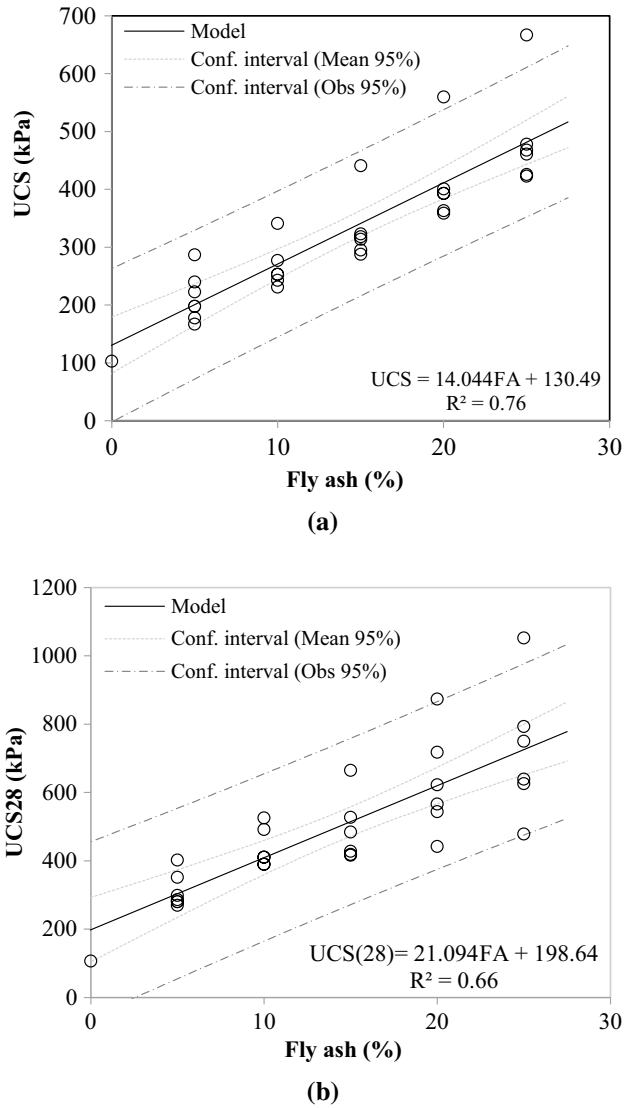

Fig. 6 Unconfined compression test results of **a** the one-day cured and **b** 28-day cured samples

The correlation coefficients of multiple regression analyses made for estimating the UCS values of the one-day cured samples were relatively lower. However, the strength predictive analysis correlation coefficient of 28-day cured specimens was higher because the one-day cured UCS values were also used in these analyses (Table 8).

In this study, ternary diagrams were designed for the estimation of unconfined strength of soil samples mixed with fly ash. Ternary graphs are used to evaluate soil strength by using three different variables. Multiple regression analyses were performed in triplicate sets to investigate the relationships between variables used in the design of the ternary diagrams. The variables of fly ash content, PL, and MDD achieved the highest correlation coefficients than other triplets (Table 9).

The same analyses were tested on the triplets to predict the strength of the 28-day cured soil samples mixed with fly ash. The significance levels of the triplets showed high values when one-day cured UCS1 values were added to the list of variables (Table 10).

Further examinations were made to find the most efficient triplet variables for predicting UCS1 and UCS28. The standardised beta coefficient-dependent variable compares the power of each independent variable (Figs. 7, 8). The high absolute value of the beta coefficient has a dominant effect. For instance, a beta of 0.89 of UCS1 has a stronger impact

Table 5 Changes in the physical and mechanical behaviour of soil samples containing 25% fly ash (the negative values indicate a decrease)

Fly ash type	% Variation in geomechanical properties							
	ΔLL	ΔPL	ΔPI	ΔAc	ΔOMC	ΔMDD	ΔUCS1	ΔUCS28
YFA	− 17.8	22.4	− 36.2	− 36.2	30.5	− 16.1	364.1	490.0
CFA	− 24.2	17.1	− 43.1	− 42.9	18.9	− 23.6	354.4	607.7
SeFA	− 17.9	15.1	− 33.0	− 32.4	21.6	− 16.2	347.6	648.1
OFA	− 16.6	14.2	− 30.7	− 30.5	10.9	− 4.3	310.7	502.8
SFA	− 13.6	16.8	− 27.5	− 26.7	39.3	− 23.8	547.4	892.8
TFA	− 9.7	29.5	− 27.8	− 27.6	17.8	− 5.4	313.6	351.0

ΔLL difference in liquid limit, *ΔPL* difference in plastic limit, *ΔPI* changes in plasticity index, ΔA_c changes in clay activity, *ΔOMC* optimum water content, *ΔMDD* changes in the maximum dry density, *ΔUCS1* uniaxial compressive strength of the one-day cured samples, and *ΔUCS28* compressive strength of the 28-day cured fly ash–soil mix

Table 6 Statistical evaluation of the variables (including seventeen studies from the literature)

Variables	Min	Max	$\bar{x}$	σ	CoV(%)	n
FA (%)	0	100	17	–	–	122
PL (%)	9.25	63.4	30.09	11.36	37.8	122
LL (%)	24	228	65.23	29.44	45.1	122
A_c	0.13	2.11	0.63	0.37	57.8	122
OMC (%)	12.0	40.98	25.08	6.96	27.7	122
MDD (kN/m^3)	12.0	20.01	14.62	1.68	11.5	122
UCS1 (kPa)	25	410	216	91.37	42.3	122
UCS28 (kPa)	27.8	622.3	300.9	127.8	42.5	122

FA fly ash, *LL* liquid limit, *PL* plastic limit, A_c clay activity, *OMC* optimum water content, *MDD* the maximum dry density, *UCS1* uniaxial compressive strength of the one-day cured samples, *UCS28* compressive strength of the 28-day cured fly ash–soil mix, $\bar{x}$ mean, σ standard deviation, *CoV* coefficient of variance, and n number of tests

Table 7 Model equations

Model no.	Equation
1	UCS1 = 1009.18 − 2.92*FA − 0.12*LL + 0.38*PL − 85.94*Ac − 5.57*OMC − 37.86*MDD
2	UCS28 = 1476.85 − 3.81*FA − 0.93*LL + 1.01*PL − 56.61*Ac − 7.38*OMC − 58.89*MDD
3	UCS28 = 221.15 − 0.18*FA − 0.77*LL + 0.54*PL + 50.33*Ac − 0.45*OMC − 11.78*MDD + 1.24*UCS1

FA fly ash%, *LL* liquid limit%, *PL* plastic limit%, A_c clay activity, *OMC* optimum water content%, and *MDD* maximum dry unit weight (kN/m^3)

Table 8 Variables and the goodness of fit statistics

Model no.	Parameters	R^2	MAPE	RMSE	Estimated
1	FA, LL, PL, A_c, OMC, and MDD	0.52	40.342	65.002	UCS1
2	FA, LL, PL, A_c, OMC, and MDD	0.5	43.106	92.782	UCS28
3	FA, LL, PL, A_c, OMC, MDD, and UCS1	0.88	12.501	45.66	UCS28

FA fly ash, *LL* liquid limit, *PL* plastic limit, A_c clay activity, *OMC* optimum water content, and *MDD* maximum dry unit weight, *UCS1* compressive strength of the one-day cured fly ash–soil mix and R^2 correlation coefficient, *UCS28* compressive strength of 28-day cured fly ash–soil mix, *MAPE* mean absolute percentage error, *RMSE* root mean square error

Table 9 Relationship between the variables and UCS of the one-day cured samples

FA	LL	PL	A_c	MDD	OMC	R^2
x	x		x			0.247
x		x	x			0.225
x	x				x	0.166
x		x			x	0.167
x			x		x	0.225
x				x	x	0.404
x	x			x		0.361
x		x		x		0.406
x			x	x		0.304

R^2 correlation coefficient

Table 10 Relationship between the variables and UCS of the 28-day cured samples

FA	LL	PL	A_c	MDD	OMC	UCS1	R^2
x	x					x	0.864
x		x				x	0.864
x			x			x	0.867
x				x		x	0.872
x					x	x	0.865
x	x				x		0.139
x		x			x		0.137
x			x		x		0.167
x	x			x			0.388
x		x		x			0.333
x			x	x			0.388

FA fly ash, *LL* liquid limit, *PL* plastic limit, A_c clay activity, *OMC* optimum water content, and *MDD* maximum dry unit weight, *UCS1* compressive strength of the one-day cured fly ash–soil mix, and R^2 correlation coefficient

than a beta of 0.144 of PL (Fig. 8). Standard beta coefficients have a standard deviation as a unit. The meaning of those variables can easily be compared with each other. In regression analysis, different groups and different scales are used, and each coefficient can be compared to the relative significance of the factors to standardise. Betas are determined by subtracting the mean from the variable and dividing by its standard deviation [50].

The PL and MDD betas showed significant effects on the UCS1 estimation (Fig. 7). Furthermore, the highest beta value belongs to UCS1 in the forecasting analysis of UCS28 (Fig. 8). As to standardised coefficients, the pair of PL and MDD was selected to estimate UCS1, and the coupling of PL and UCS1 was designated as predictive variables for UCS28 prediction.

The correlation values (r) obtained from multiple regressions (MLR) have not qualified for estimating the compressive strength values of one-day cured samples. Due to the low MLR correlation values and that ANN techniques are a better and more efficient fitting technique than MLR, ANN analyses were tested to estimate the UCS values of the one-day and 28-day cured soil specimens mixed with fly ash.

6 ANN Analyses

A neural network is an information processing system consisting of simple, highly connected nodes or processing elements with dynamic state response to external inputs [51]. The purpose of the neural network is to map a set of input patterns to the set of corresponding output models [52]. Neurocomputing architecture can be built into physical (or computational) hardware or neural software languages (or programs) that can think and act like humans [53]. Furthermore, there are many training algorithms, such as fast propagation, conjugate gradient descent, quasi-Newton, Levenberg–Marquardt, and backpropagation. However, the backpropagation method is the most commonly used algorithm in practical applications [54]. Backpropagation neural networks (BPNNs) have a layered structure with an input

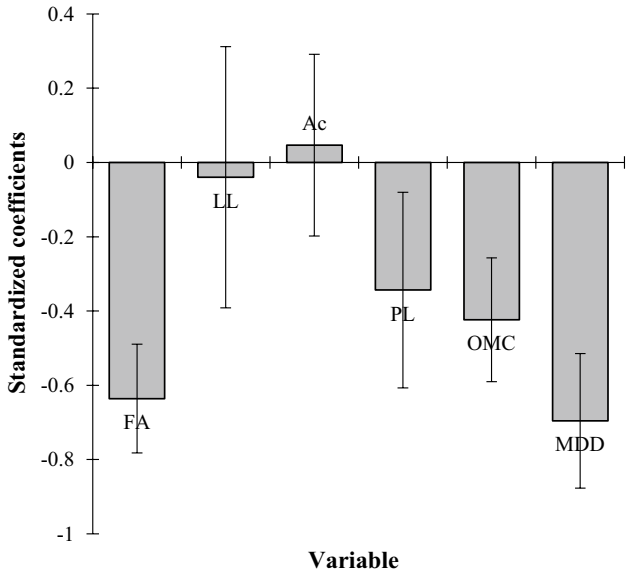

Fig. 7 Standardised coefficients of regression analysis to estimate UCS1 in 95% confidence interval (*FA* fly ash, *LL* liquid limit, *PL* plastic limit, A_c clay activity, *OMC* optimum water content, and *MDD* maximum dry unit weight)

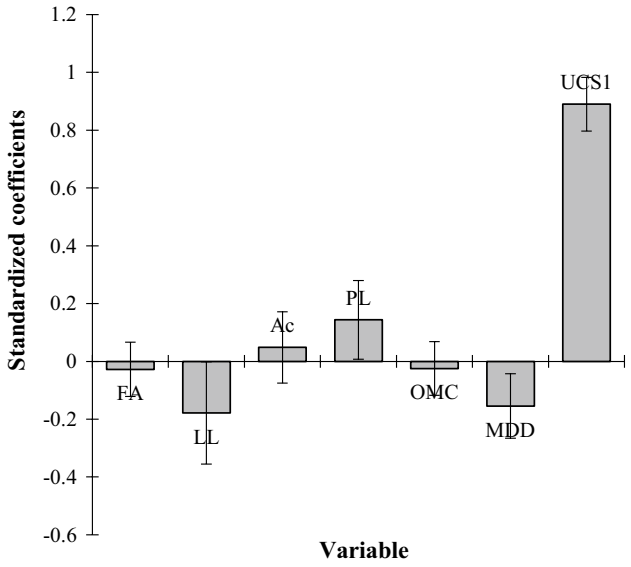

Fig. 8 Standardised coefficients of regression analysis to estimate UCS28 in 95% confidence interval (*FA* fly ash, *LL* liquid limit, *PL* plastic limit, A_c clay activity, *OMC* optimum water content, and *MDD* maximum dry unit weight, *UCS1* compressive strength of the one-day cured fly ash–soil mix)

layer and output layer, and one or more hidden layers. Further, reproduction takes place from the input layer to the output layer and compares the network outputs to known targets [55]. The learning process changes these weights by including the difference between the predicted and actual values in the matched output [56]. Each link is weighted; when the network is given a set of inputs, the associated relationships can be set to produce the desired output. Placing this weight to provide a specific output is called "training" and is the mechanism by which this system learns [57]. As implemented by [58], the desired limit uses a logistic activation function [0,1] for output transfer (Eq. 2):

$$f\left(N_j\right) = 1/\left(1 + e^{-N_j}\right) \tag{2}$$

Furthermore, the learning rate and momentum coefficient are two critical parameters that control the neural network training of the backpropagation algorithm. The learning rate is a positive constant that controls the rate at which new weight factors are set based on the calculated grade correction term. The momentum coefficient is an additional weight added to the weight factors and accelerates the adjustment rate of these weight factors [52].

Oscillation problems arise when a high value is assigned to the learning rate. However, small amounts lead to extended learning time. In the literature, values ranging from 10^{-3} to 10 have been reported to be successful in many computational backpropagation experiments [59]. The momentum coefficient also influences learning performance, which is defined as the sum of the exact ratio of the previous variation and the new change amount in the iteration. If this value is significant, a solution will be difficult to reach, and if it is small, it is difficult to eliminate a local solution. Many researchers suggested values between 0.5 and 0.8. Data scaling is an essential step in network training. One of the reasons for pre-processing the output data is the use of a sigmoidal transfer function in the network. The upper and lower limits of the output from the sigmoid transfer function are usually one and zero, respectively [60, 61]. Scaling the entries to the range $[-1, +1]$ improves the learning rate dramatically because these values fall into the region of the sigmoid transfer function that is most sensitive to variants of the input values to the outputs [60]. The type of data scaling depends on the data distribution. A simple linear normalisation function for the values of 0–1 is shown as (Eq. 3):

$$V_n = \left(V_s - V_{min}\right) / \left(V_{max} - V_{min}\right) \tag{3}$$

where V_n is the normalised value, V_{min} and V_{max} are the minimum and maximum values, and V_s is the source (denormalised) value.

The ANN analyses were tested using all variables to estimate the unconfined strength of one-day cured samples. Before examination, the data files were divided into two groups: the first set is used as a test set contained 70% of the data, and the second set is used as a validation set consisting of 30% of the data. The percentage of training data should be kept high to find the correct solution. For this reason, the partition ratio for this cluster was defined as 70%. Moreover,

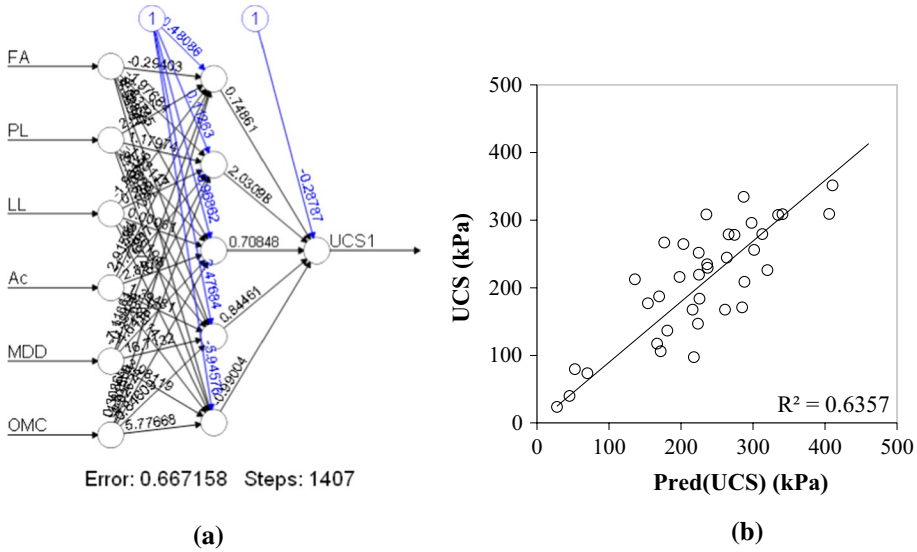

Fig. 9 **a** Neural network model for the estimation of UCS. **b** The relationship between predicted data of unconfined compressive strength of FA mixed soil and test data (*FA* fly ash, *LL* liquid limit, *PL* plastic limit, A_c clay activity, *OMC* optimum water content, and *MDD* maximum dry unit weight, *UCS1* compressive strength of the one-day cured fly ash–soil mix)

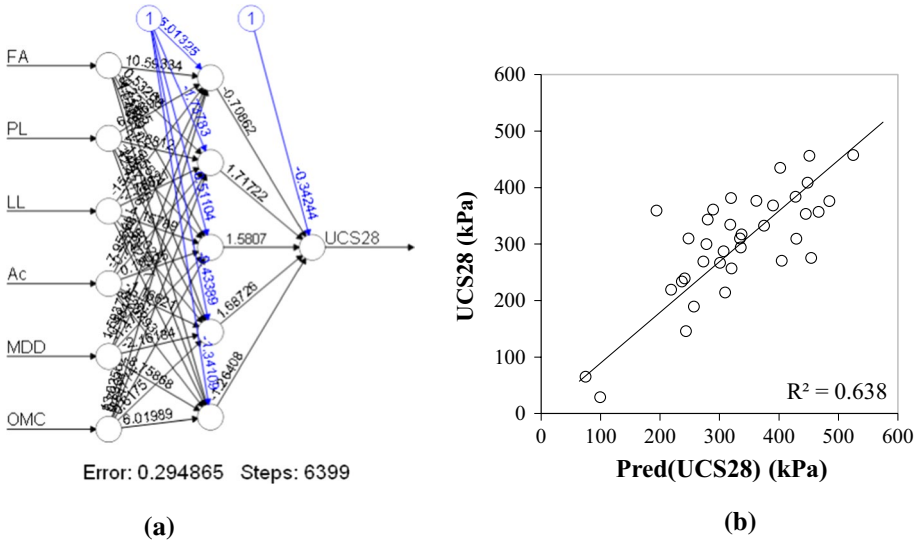

Fig. 10 **a** Network of the training data and **b** the relationship between real and predicted data of the 28-day cured samples mixed FA (without UCS1 variable) (*FA* fly ash, *LL* liquid limit, *PL* plastic limit, A_c clay activity, *OMC* optimum water content, and *MDD* maximum dry unit weight)

the data from all the sets were randomly selected from the data list, and Eq. 2 was used to normalise the data.

In the neural model, a flexible backpropagation (Rprop) learning algorithm with five neurons was used in the hidden layer. Six parameters were selected in the input layer: FA, PL, LL, A_c, MDD, and OMC (Fig. 9a). The unconfined strength values (UCS1) of one-day cured samples were also selected in the output layer. Finally, they successfully predicted the output data. The RMSE value of the test procedure was found to be 48.32. Similarly, the correlation coefficient ($R^2 = 0.636$) indicated the accuracy of the predicted model (Fig. 9b).

Furthermore, the same ANN method and the number of neurons were used to estimate the strength of the 28-day cured samples (Fig. 10a, b). For test data, the RMSE value was calculated as 49.52 and the R^2 value between the actual and predicted data was 0.638.

Low RMSE (for testing data: 29.55) as well as relatively higher correlation coefficient value ($R^2 = 0.826$) was obtained when the UCS1 variant was used to estimate the strength of the 28-day cured specimens (Fig. 11a, b). One-day cured specimen strength (UCS1) is an essential parameter in assessing the unconfined strength of cured samples (UCS28).

Neural networks are typically arranged in layers consisting of a series of interconnected ``nodes'' that contain an ``activation function''. The patterns are applied to the network through an ``input layer'' that communicates with one or more ``hidden layers'' through which the actual processing is performed via a weighted ``links'' system. Most ANNs include a sort of "learning rule" that changes the weights of links according to the input models provided. Although there are many different learning rules used by neural networks, this study is only about one: delta rule. The

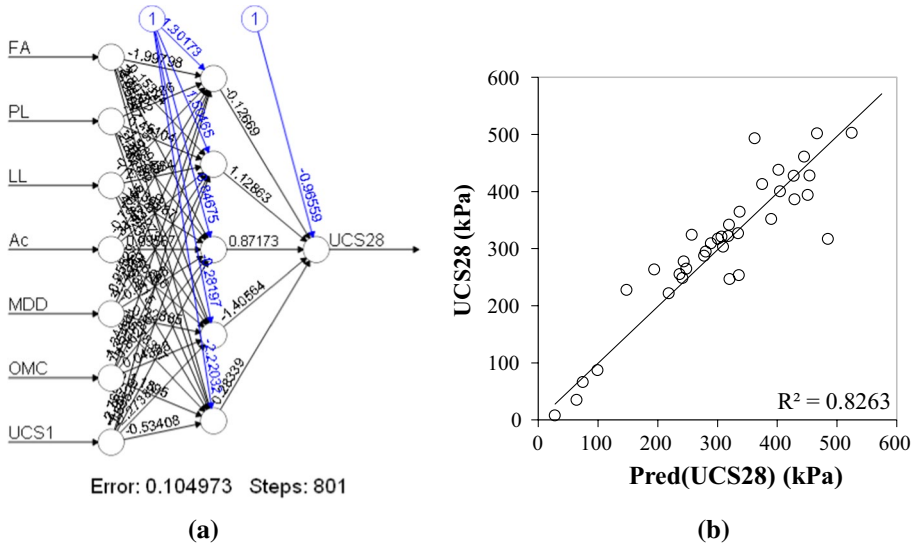

Fig. 11 **a** Network of the test data and **b** the relationship between real and predicted data of the 28-day cured samples mixed FA (within UCS1 variable) (*FA* fly ash, *LL* liquid limit, *PL* plastic limit, A_c clay activity, *OMC* optimum water content, and *MDD* maximum dry unit weight, *UCS1* compressive strength of the one-day cured fly ash–soil mix)

delta rule is usually used by the most common YSA class BPNNs. For other types of backpropagation, "learning" is a controlled process that occurs when the outputs are moved forward in each cycle or at the time when the network is presented with a new entry model and by backward propagation of weight settings.

The hidden layers are required when the neural network needs to understand something that is complex, contextual, or unclear, such as image recognition. "Deep" learning comes from having many hidden layers. These layers are known as "hidden" because they cannot be seen as network outflows. The synapses take the input and multiply it by a "weight" (the "strength" of the input in the output determination). The neurons add the output from all synapses and apply an activation function. Training a neural network means calibrating all the "weights" by repeating two basic steps, forward propagation and backpropagation. In forward propagation, the input data are applied to a set of weights and outputs. For the first forward propagation, the weight set is selected randomly. Neural networks repeat both forward and backward propagation until the weights are calibrated to accurately predict an output. The calculation of the incremental change in these weights takes place in two steps: (1) the subtraction of the difference of weights by multiplying the cumulative output of the delta output by the cumulative output (called the delta output) and (2) find the error margin of the output result. At the end of iterations, the weights of a network, including five neurons, were determined for estimating UCS1 (Table 11).

The weights and intercepts of the network for estimating the strength of cured samples (UCS28) were calculated and are presented in Tables 12 and 13. The UCS1 was used as a predictive variable in the last ANN analyses (Table 13) for estimating UCS28.

Table 11 Weights of the artificial network for one-day cured samples strength (UCS1)

Weights of/ neuron no.	1	2	3	4	5	
Intercept	0.481	0.113	−0.969	3.477	−5.946	
FA	−0.294	−1.977	−3.837	6.029	4.586	
PL	2.429	1.180	−1.431	−5.187	21.926	
LL	−1.956	0.269	0.001	−8.862	−0.997	
Ac	2.916	−1.779	2.898	1.395	5.243	
MDD	−7.117	−0.394	−4.642	16.713	3.081	
OMC	0.309	−1.818	−0.026	0.846	5.777	Intercept
To UCS1	0.749	2.031	0.708	0.845	−0.990	−0.288

FA fly ash, *LL* liquid limit, *PL* plastic limit, A_c clay activity, *OMC* optimum water content, *MDD* maximum dry density, *UCS1* uniaxial compressive strength of the one-day cured sample, *UCS28* compressive strength of the 28-day cured fly ash–soil mix

7 Ternary Diagrams

A ternary plot or triangle graph is a barycentric graph of three variables that sum to a constant. The ratios of the three variables are equilateral triangular locations as a graph. It is used to show the compositions of systems used in physical chemistry, petrology, mineralogy, metallurgy, and other physical sciences. In a ternary plot, the proportions of the three variables a, b, and c must sum up to some constant K, which is defined as 1.0 or 100%. As $a+b+c=K$ for all the items in the graph, no variable is independent of the others. Therefore, only two variables must be known to find a sample point in the chart: for example, c must be equal to $K-a-b$. The three proportions cannot change

Table 12 Weights of the artificial network for cured samples strength (UCS28)

Weights of/neuron no.	1	2	3	4	5	
Intercept	−5.013	−1.738	0.511	−0.434	−1.341	
FA	10.593	0.533	−0.229	−4.314	−11.488	
PL	6.087	2.268	−1.256	14.478	42.432	
LL	−15.495	−2.758	−4.158	−0.800	−12.422	
A_c	−7.957	−0.730	0.109	−1.166	3.283	
MDD	1.594	−0.484	−1.475	−2.162	−8.759	
OMC	13.026	0.736	0.848	0.617	6.020	Intercept
To UCS28	−0.709	1.717	1.581	1.687	−1.264	−0.342

FA fly ash, *LL* liquid limit, *PL* plastic limit, A_c clay activity, *OMC* optimum water content, *MDD* the maximum dry density, *UCS1* uniaxial compressive strength of the one-day cured sample, *UCS28* compressive strength of the 28-day cured fly ash–soil mix

Table 13 Weights of the artificial network for cured samples strength (UCS28) with UCS1

Weights of/neuron no.	1	2	3	4	5	
Intercept	1.302	1.505	0.847	−0.282	−2.220	
FA	−1.998	−0.153	2.807	2.358	3.950	
PL	−0.443	0.451	−1.989	−1.394	2.884	
LL	−0.441	2.910	−3.396	−0.233	4.642	
A_c	−0.778	34.939	0.096	0.567	5.634	
MDD	−0.955	4.743	−0.418	−0.229	−5.784	
OMC	−1.345	7.355	−0.863	0.044	1.190	
UCS1	−2.769	−4.957	1.595	−2.274	−0.534	Intercept
To UCS28	−0.127	1.129	0.872	−1.406	0.283	−0.966

FA fly ash, *LL* liquid limit, *PL* plastic limit, A_c clay activity, *OMC* optimum water content, *MDD* the maximum dry density, *UCS1* uniaxial compressive strength of the one-day cured samples, *UCS28* compressive strength of the 28-day cured fly ash–soil mix

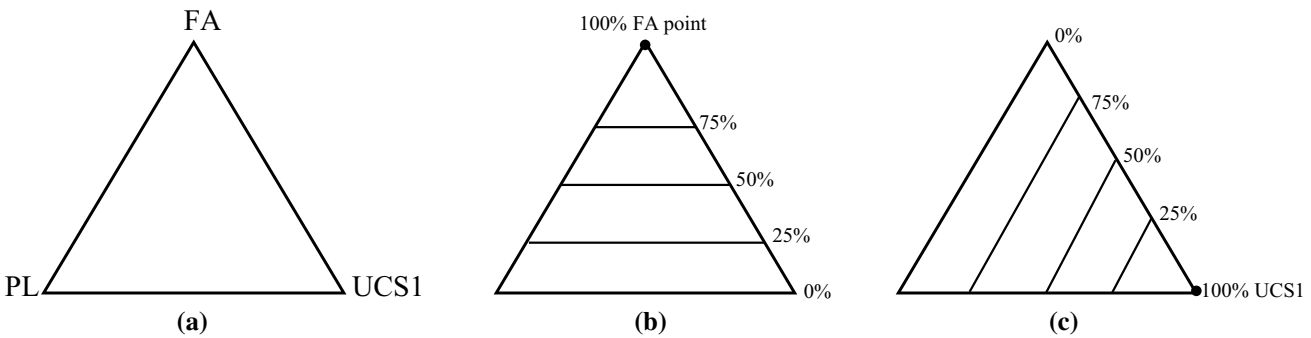

Fig. 12 Ternary plot explanation. **a** Example ternary diagram without any points plotted, **b** showing increases along the first axis and **c** presenting increments along the third axis

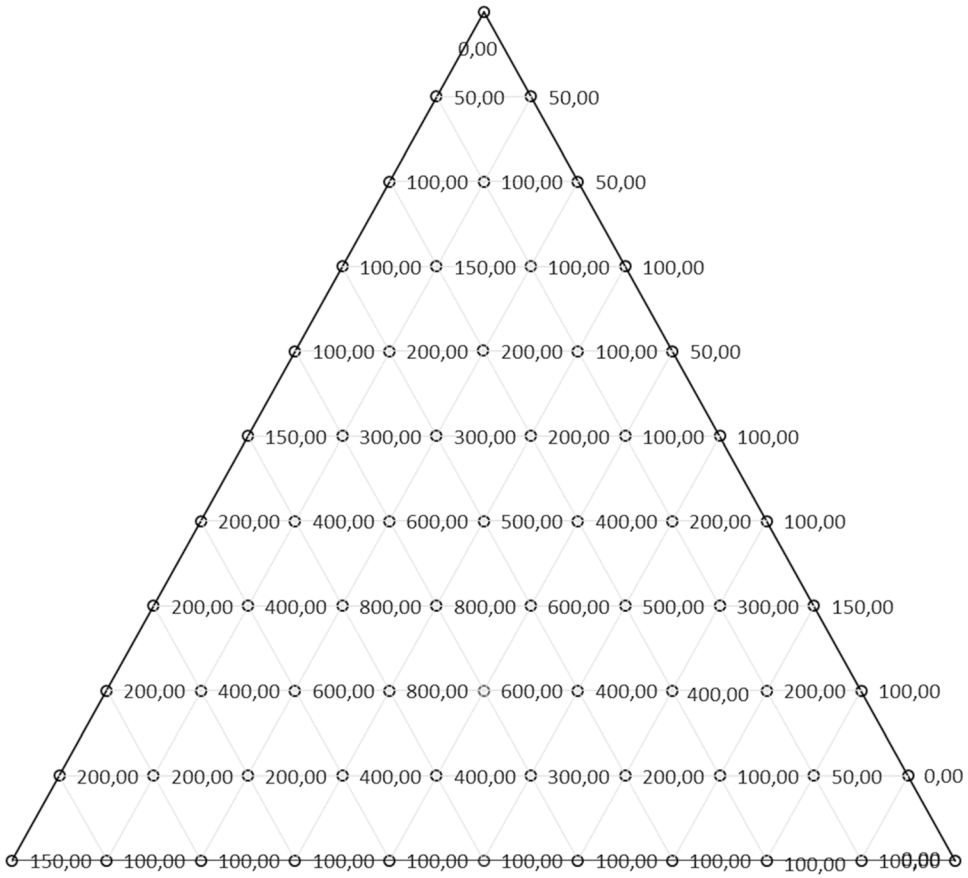

Fig. 13 Example displays of the ternary plots

independently. There are only two degrees of freedom, and it is possible to plot. The advantage of using a triple plot to describe the compositions is that the three variables can easily be plotted in a two-dimensional plot. Triplets can also be used to generate phase diagrams by summarising form regions on a line containing different aspects. Each point on the triplet represents a distinct combination of the three components. As shown in Fig. 12, the percentage of a particular creep decreases linearly with increasing distance from this corner. Fine lines can be created to quickly estimate the content of a range by drawing lines parallel at regular intervals (as seen in the images) between the zero edge and corner.

The ANN analyses were utilised to create the triangular diagrams. When the triangular diagrams are constructed, the sum of the x, y, and z components of a point on the abacus must be one or 100. One- and 28-day strengths of the fly ash–soil mixtures were estimated for each aspect of the abacus by the ANN software using triple changers. The image showing the ternary chart plots is shown in Fig. 13. A contour graph was created by combining the points of the ternary graph. MATLAB 2016 software [62] was used for forming the ternary contour diagrams.

A triplet was constructed according to the significance of the variables, and the triangular abacus was developed. The MDD and PL variables having a high significance level were chosen for the first trilateration. The maximum and minimum values of variables were used as axis limiters in the ternary charts (Fig. 14). The linear relationship between the strength and observed values of the one-day cured specimens estimated in the ternary diagram was determined. The correlation coefficient (R^2) between the predicted and the original data is 0.60 (Fig. 15).

Other triplets were designed for estimating the compressive strengths of the 28-day cured samples. The first ternary chart consisted of the UCS values of one-day cured samples (UCS1) and the PL values of soils (Fig. 16). The maximum strength values of the 28-day cured samples gathered around 22% fly ash content and 21% of PL. Sometimes, three values are not shown as a triple junction on the chart. In this case, the UCS1 and FA values must be used for estimating the UCS28 of the samples first. The PL value can be used if the UCS1 value was located at the corner. The predicted data obtained from the ternary graph were compared with the original data (Fig. 17). It has presented a reasonable result ($R^2 = 0.84$).

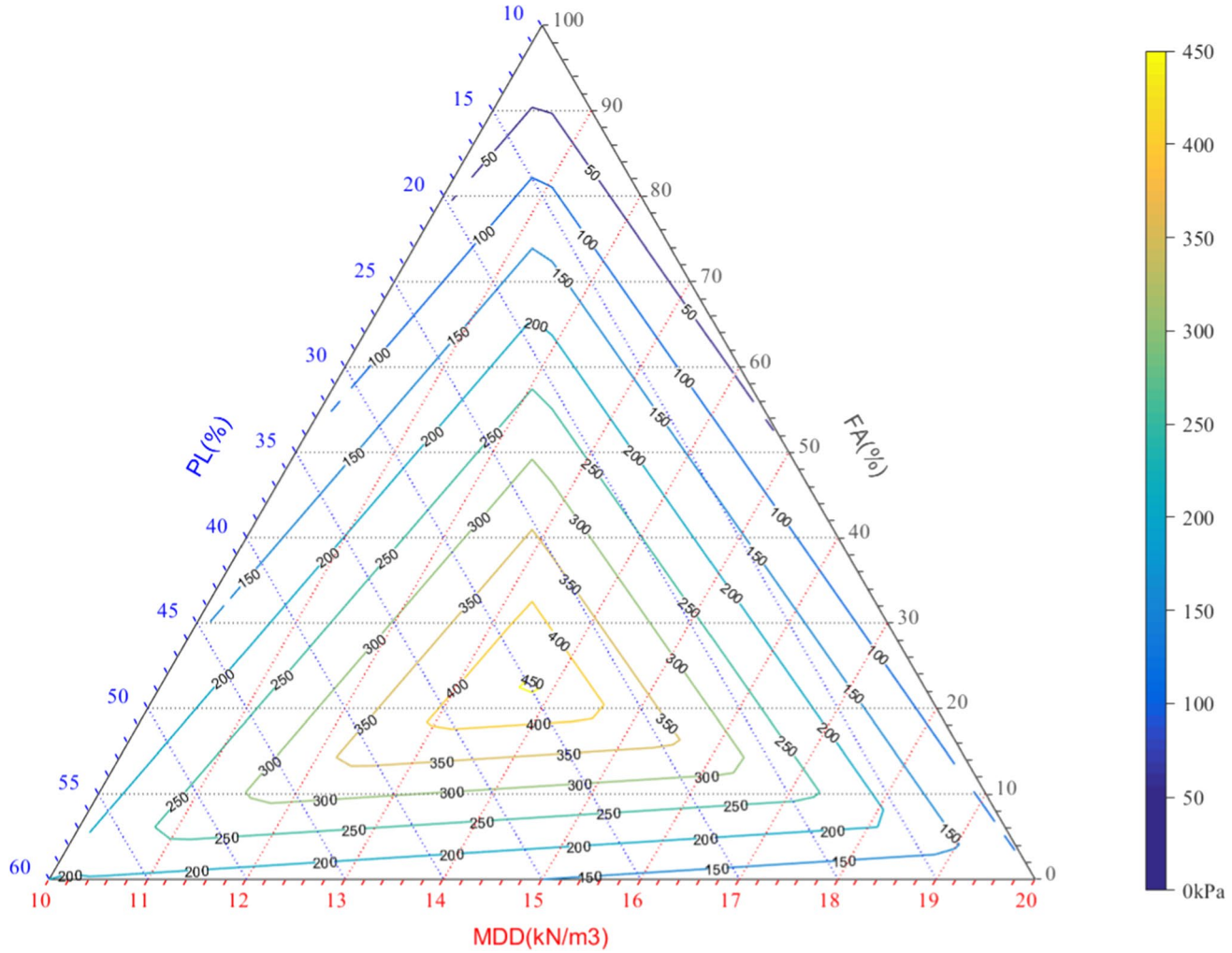

Fig. 14 Ternary diagram for estimating unconfined compressive strength by using data of the max dry unit weight of Proctor test (MDD) fly ash content (FA) and PL

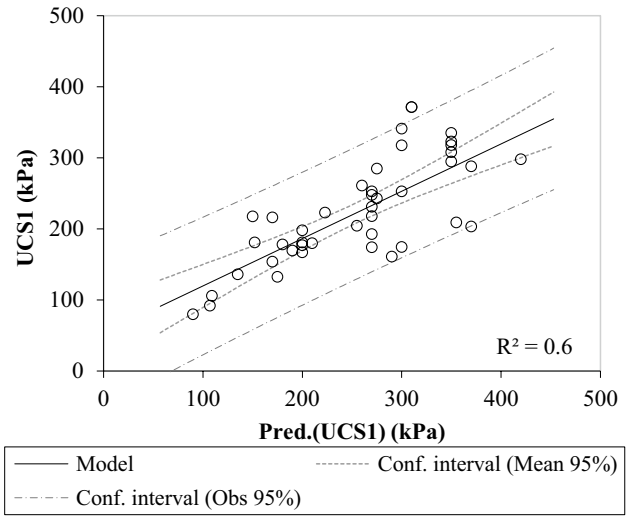

Fig. 15 Performance of the ternary chart: the relationship between the real data and that predicted for UCS1

8 Conclusions

The following conclusions were drawn based on the work reported in this study:

(1) The MDD values of the soil samples decreased from 4 to 23% depending on the fly ash content. The reason is that the fly ash density is low, and the unit weight value of the mixture decreases with the increased fly ash content in the soil as well as the DDL thickness decreasing with the use of fly ash, causing clay particle flocculation. This flocculation generates a resistance against the compaction effort, which causes an MDD reduction.

(2) The fly ash addition affected the strength and physical properties of the soil in a positive direction. The maximum strength increase was determined in the sam-

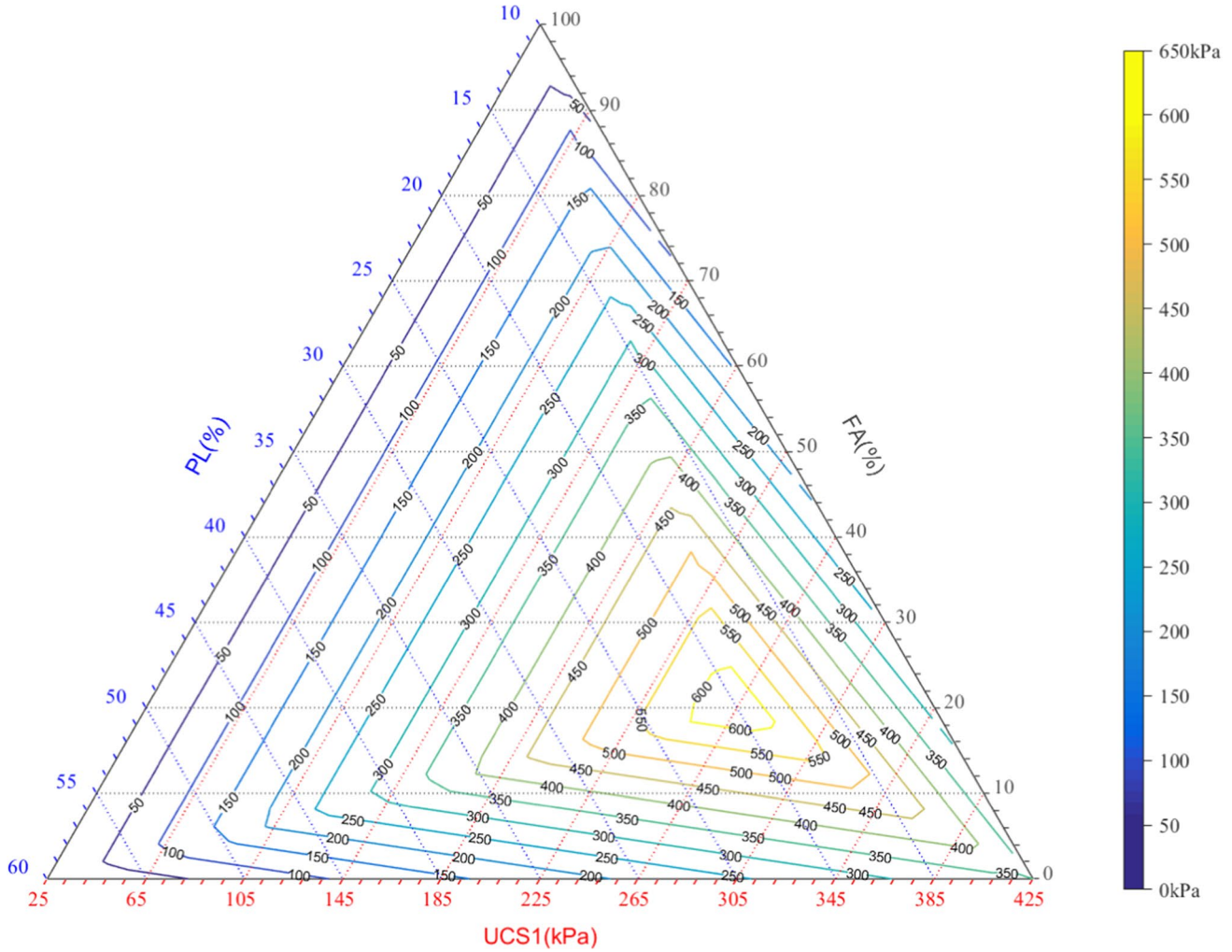

Fig. 16 Ternary chart for estimating the unconfined compressive strength of the 28-day cured samples using UCS1 and PL data

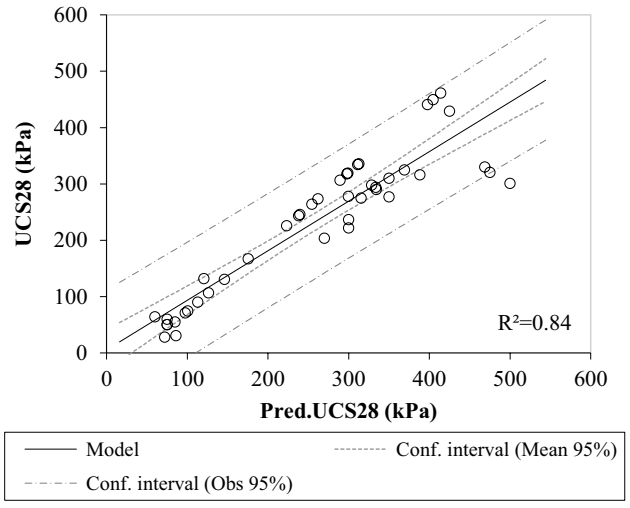

Fig. 17 Performance of the ternary chart: the relationship between the actual data and that predicted for UCS28

ples with SFAs (547.4%) and the least improvement in strength with OFAs (310.7%).

(3) The dataset in this study was evaluated together with those from seventeen other studies in the literature. The physical and mechanical properties for samples with 0–100% fly ash content were assessed. Using the Atterberg limit values, proctor test results, and UCS values of the fly ash samples, an attempt was made to estimate the resistance values of the cured and one-day cured samples of the fly ash samples by multiple regression and ANN analyses. In MLR, the predictive value of the correlation coefficient (R^2) of the one-day cured specimens was 0.52. The highest correlation ($R^2 = 0.88$) in the strength prediction equations of 28-day cured samples was observed in the MLR analyses, in which the durability values of the one-day cured samples were used as variables.

(4) The ANN analyses were performed because the correlation coefficients of the prediction equations in the MLR

determination are low. Furthermore, the neural weights of ANN analyses, which gave the highest correlation, were determined.

(5) The estimated UCS values, obtained using the ternary prediction graphs, were compared with the actual data, and the estimation capacity of the ternary diagrams was evaluated. The correlation coefficient (R^2) between the original data and values estimated from a ternary graph of the one-day cured specimens is 0.6. Further, the estimation of 28-day cured samples showed $R^2 = 0.84$.

References

1. Kaplan, G.; Gultekin, A.B.: The investigation of fly ash usage in terms of environmental and social effects in construction sector. In: Proceeding of the International Sustainable Buildings Symposium (ISBS), 26–28 May 2010, Ankara, Turkey (Turkish) (2010)
2. Turhan, S.; Parmaksiz, A.; Köse, A.; Yüksel, A.; Arikan, I.H.; Yücel, B.: Radiological characteristics of pulverized fly ashes produced in Turkish coal-burning thermal power plants. Fuel **89**(12), 3892–3900 (2010). https://doi.org/10.1016/j.fuel.2010.06.045
3. Xu, H.; Van Deventer, J.S.J.: The geopolymerisation of aluminosilicate minerals. Int. J. Miner. Process. **59**(3), 247–266 (2000). https://doi.org/10.1016/S0301-7516(99)00074-5
4. Khale, D.; Chaudhary, R.: Mechanism of geopolymerization and factors influencing its development: a review. J. Mater. Sci. **42**(3), 729–746 (2007). https://doi.org/10.1007/s10853-006-0401-4
5. Mozumder, R.A.; Laskar, A.I.: Prediction of unconfined compressive strength of geopolymer stabilized clayey soil using artificial neural network. Comput. Geotech. **69**, 291–300 (2015). https://doi.org/10.1016/j.compgeo.2015.05.021
6. Mackiewicz, S.M.; Ferguson, E.W.: Stabilization of soil with self-cementing coal ashes. In: Proceedings of the World of Coal Ash (WOCA'05). Lexington (2005)
7. Binal, A.: The effects of high alkaline fly ash on strength behaviour of a cohesive soil. Adv. Mater. Sci. Eng. (2016). https://doi.org/10.1155/2016/3048716
8. Ferguson, G.: Use of self-cementing fly ash as a soil stabilizing agent. Fly ash for soil improvement. GSPno. 36, ASCE Geotechnical Special Publication (1993)
9. Misra, A.: Stabilization characteristics of clays using Class C fly ash. Transp. Res. Rec. **1611**(1), 46–54 (1998). https://doi.org/10.3141/1611-06
10. Puppala, A.J.; Musenda, C.: Effects of fiber reinforcement on strength and volume change in expansive soils. Transp. Res. Rec. **1736**, 134–140 (2000). https://doi.org/10.3141/1736-17
11. Prabakar, J.; Dendorkar, N.; Morchhale, R.K.: Influence of fly ash on strength behavior of typical soils. Constr. Build. Mater. **18**(4), 263–267 (2004). https://doi.org/10.1016/j.conbuildmat.2003.11.003
12. Gumuser, C.; Senol, A.: Effect of fly ash and different lengths of polypropylene fibers content on the soft soils. IJCE **12**(2 and B), 134–145 (2014)
13. Bin-Shafique, S.; Rahman, K.; Yaykiran, M.; Azfar, I.: The long-term performance of two fly ash stabilized fine-grained soil subbases. Resour. Conserv. Recycl. **54**(10), 666–672 (2010). https://doi.org/10.1016/j.resconrec.2009.11.007
14. Nicholson, P.G.; Kashyap, V.: Fly ash stabilization of tropical Hawaiian soils in fly ash for soil improvement. ASCE Geotech. Spec. Publ. **36**, 1134–1147 (1993)
15. Kolias, S.; Kasselouri-Rigopoulou, V.; Karahalios, A.: Stabilisation of clayey soils with high calcium fly ash and cement. Cem. Concr. Compos. **27**(2), 301–313 (2005). https://doi.org/10.1016/j.cemconcomp.2004.02.019
16. Du, Y.; Li, S.; Hayashi, S.: Swelling-shrinkage properties and soil improvement of compacted expansive soil, Ning-Liang Highway, China. Eng. Geol. **53**(3–4), 351–358 (1999). https://doi.org/10.1016/S0013-7952(98)00086-6
17. Langroudi, A.A.; Yasrobi, S.S.: A micro-mechanical approach to swelling behavior of unsaturated expansive clays under controlled drainage conditions. Appl. Clay Sci. **45**(1–2), 8–19 (2009). https://doi.org/10.1016/j.clay.2008.09.004
18. Lin, D.-F.; Lin, K.-L.; Hung, M.-J.; Luo, H.-L.: Sludge ash/hydrated lime on the geotechnical properties of soft soil. J. Hazard. Mater. **145**(1–2), 58–64 (2007). https://doi.org/10.1016/j.jhazmat.2006.10.087
19. Nalbantoglu, Z.: Effectiveness of class C fly ash as an expansive soil stabilizer. Constr. Build. Mater. **18**(6), 377–381 (2004). https://doi.org/10.1016/j.conbuildmat.2004.03.011
20. Yong, R.N.; Ouhadi, V.R.: Experimental study on instability of bases on natural and lime/cement-stabilized clayey soils. Appl. Clay Sci. **35**(3–4), 238–249 (2007). https://doi.org/10.1016/j.clay.2006.08.009
21. Kang, X.; Ge, L.; Kang, G.-C.; Mathews, C.: Laboratory investigation of the strength, stiffness, and thermal conductivity of fly ash and lime kiln dust stabilised clay subgrade materials. Road Mater. Pavement Des. **16**(4), 928–945 (2015). https://doi.org/10.1080/14680629.2015.1028970
22. Sukmak, P.; Horpibulsuk, S.; Shen, S.-L.; Chindaprasirt, P.; Suksiripattanapong, C.: Factors influencing strength development in clay–fly ash geopolymer. Constr. Build. Mater. **47**, 1125–1136 (2013). https://doi.org/10.1016/j.conbuildmat.2013.05.104
23. Wang, Y.; Zhang, M.H.; Li, W.; Chia, K.S.; Liew, J.Y.R.: Stability of cenospheres in lightweight cement composites in terms of alkali-silica reaction. Cem. Concr. Res. **42**, 721–727 (2012). https://doi.org/10.1016/j.cemconres.2012.02.010
24. Hanif, A.; Lu, Z.; Diao, S.; Zeng, X.; Li, Z.: Properties investigation of fiber reinforced cement-based composites incorporating cenosphere fillers. Constr. Build. Mater. **140**, 139–149 (2017). https://doi.org/10.1016/j.conbuildmat.2017.02.093
25. Toktas, F.: Behavior and stabilization of dispersive soils with C type fly ash. Dissertation, Middle East Technical University, Ankara, Turkey (2001)
26. ASTM C618: Standard specification for coal fly ash and raw or calcined natural pozzolan for use in concrete. American Society for Testing and Materials, West Conshohocken, PA, USA (2010)
27. TUBITAK: Production of Synthetic Zeolites in Laboratory and Pilot Scales from Fly Ashes in Turkish Coal-Fired Power Plants. Project Manager:Ali İhsan Karayigit, Project No: 105M274, Ankara, Turkey **(in Turkish)** (2009)
28. ASTM D7762: Standard Practice for Design of Stabilization of Soil and Soil-Like Materials with Self-Cementing Fly Ash. American Society for Testing and Materials, West Conshohocken, PA, USA (2011)
29. ASTM D698: Standard Test Methods for Laboratory Compaction Characteristics of Soil Using Standard Effort (12 400 ft-lbf/ft3 (600 kN-m/m^3)). American Society for Testing and Materials, West Conshohocken, PA, USA (2010)
30. Ismaiel, H.A.H.: Treatment and improvement of the geotechnical properties of different soft fine grained soils using chemical

stabilization. Dissertation, Martin Luther Universität, Halle-Wittenberg, Germany (2006)
31. Sezer, A.; Inan, G.; Yılmaz, H.R.; Ramyar, K.: Utilization of a relatively higher lime fly ash for improvement of Izmir clay. Build. Environ. **41**(2), 150–155 (2006). https://doi.org/10.1016/j.buildenv.2004.12.009
32. Reyes, A.; Pando, M.: Evaluation of CFBC fly ash for improvement of soft clays. In: Proceedings of the World of Coal Ash (WOCA), Covington, Kentucky, USA (2007). https://doi.org/10.1007/s00521-017-3305-0
33. Aksoy H.S.; Yılmaz M.; A.E.E.: Stabilization of a clayey soil with Tunçbilek fly ash. Fırat Univ. Dogu Anadolu Bolgesi Arastirmalari Derg. **6**, 88–92 (2008)
34. Brooks, R.; Udoeyo, F.F.; Takkalapelli, K.V.: Geotechnical properties of problem soils stabilized with fly ash and limestone dust in Philadelphia. J. Mater. Civ. Eng. ASCE **23**(5), 711–716 (2011). https://doi.org/10.1061/(ASCE)MT.1943-5533.0000214
35. Sai, D.T.R.; Shankar,; Naik, M.: Influence of fly ash on the strength behaviour of lime and cement treated red soil. Int. J. Environ. Res. Dev. **4**(2), 135–140 (2014)
36. Firat, S.; Khatib, J.M.; Yilmaz, G.; Comert, A.: Effect of curing time on selected properties of soil stabilized with fly ash, marble dust and waste sand for road sub-base materials. Waste Manag. Res. **35**(7), 747–756 (2017). https://doi.org/10.1177/0734242X17705726
37. ASTM D4318: Standard Test Methods for Liquid Limit, Plastic Limit, and Plasticity Index of Soils., West Conshohocken, PA, USA (2010)
38. ASTM D2166/D2166M: Standard test method for unconfined compressive strength of cohesive soil. American Society for Testing and Materials, West Conshohocken, PA, USA (2010)
39. Soni, N.: Influence of fly ash on the strength and swelling characteristics of bentonite. Dissertation, National Institute of Technology Rourkela, India (2010)
40. Saravanan, R.; Thomas, R.S.; Joseph, M.: A study on soil stabilization of clay soil using fly ash. Int. J. Res. Civ. Eng. Archit. Des. **1**(2), 33–37 (2013)
41. Bose, B.: Geo-engineering properties of expansive soil stabilized with fly ash. Electron. J. Geotech. Eng. **17**, 1339–1353 (2012)
42. Bhuvaneshwari, S.; Robinson, R.G.; Gandhi, S.R.: Stabilization of expansive soils using fly ash. Fly Ash India **8**, 5.1–5.10 (2005)
43. Ozdemir, M.A.: Improvement in bearing capacity of a soft soil by addition of fly ash. Procedia Eng **143**, 498–505 (2016)
44. Sharma, N.K.; Swain, S.K.; Sahoo, U.C.: Stabilization of a clayey soil with fly ash and lime: a micro level investigation. Geotech. Geol. Eng. **30**, 1197–1205 (2012). https://doi.org/10.1007/s10706-012-9532-3
45. Sivapullaiah, P.V.; Jha, A.K.: Gypsum induced strength behaviour of fly ash-lime stabilized expansive soil. Geotech. Geol. Eng. **32**(5), 1261–1273 (2014). https://doi.org/10.1007/s10706-014-9799-7
46. Zha, F.; Liu, S.; Du, Y.; Cui, K.: Behavior of expansive soils stabilized with fly ash. Nat. Hazard **47**(3), 509–523 (2008). https://doi.org/10.1007/s11069-008-9236-4
47. Kang, X.; Zhao, X.; Bate, B.: Sedimentation behavior of fly ash-kaolinite mixtures.In: International Conference on Case Histories in Geotechnical Engineering. Chicago, USA (2013)
48. Kang, X.; Xia, Z.; Chen, R.; Sun, H.; Yang, W.: Effects of inorganic ions, organic polymers, and fly ashes on the sedimentation characteristics of kaolinite suspensions. Appl. Clay Sci. **181**, 105220 (2019). https://doi.org/10.1016/j.clay.2019.105220
49. Montgomery, D.C.; Runger, G.C.: Applied statistics and probability for engineers. Wiley, New York (1999)
50. Freedman, D.A.: Statistical Models: Theory and Practice, 2nd edn. Cambridge University Press, Cambridge (2009)
51. Hecht-Nielsen, R.: Neurocomputing. Addison-Wesley, Missouri (1990)
52. Baughman, D.R.; Liu, Y.: Neural networks in bio-processing and chemical engineering. Academic Press, New York (1995)
53. Oztas, A.; Pala, M.; Ozbay, E.; Kanca, E.; Cağlar, N.; Bhatti, M.A.: Predicting the compressive strength and slump of high strength concrete using neural network. Constr. Build. Mater. **20**(9), 769–775 (2006). https://doi.org/10.1016/j.conbuildmat.2005.01.054
54. Marti, R.; El-Fallahi, A.: Multilayer neural networks: an experimental evaluation of on-line training methods. Comput. Oper. Res. **31**(9), 1491–1513 (2004). https://doi.org/10.1016/S0305-0548(03)00104-7
55. Kewalramani, M.A.; Gupta, R.: Concrete compressive strength prediction using ultrasonic pulse velocity through artificial neural networks. Automat. Constr. **15**(3), 374–379 (2006). https://doi.org/10.1016/j.autcon.2005.07.003
56. Yang, Y.; Rosenbaum, M.S.: The artificial neural network as a tool for assessing geotechnical properties. Geotech. Geol. Eng. **20**(2), 149–168 (2002). https://doi.org/10.1023/A:1015066903985
57. Pala, M.; Ozbay, E.; Oztas, A.; Yuce, M.I.: Appraisal of long-term effects of fly ash and silica fume on compressive strength of concrete by neural networks. Constr. Build. Mater. **21**(2), 384–394 (2007). https://doi.org/10.1016/j.conbuildmat.2005.08.009
58. Neaupane, K.M.; Achet, S.H.: Use of backpropagation neural network for landslide monitoring: a case study in the higher Himalaya. Eng. Geol. **74**(3–4), 213–226 (2004). https://doi.org/10.1016/j.enggeo.2004.03.010
59. Zurada, M.J.: Introduction to artificial neural systems. PWS, Boston (1992)
60. Rafiq, M.Y.; Bugmann, G.; Easterbrook, D.J.: Neural network design for engineering applications. Comput. Struct. **79**(17), 1541–1552 (2001). https://doi.org/10.1016/S0045-7949(01)00039-6
61. Binal, A.: Prediction of mechanical properties of non-welded and moderately welded ignimbrite using physical properties, ultrasonic pulse velocity, and point load index tests. Q. J. Eng. Geol. Hydrogeol. **42**(1), 107–122 (2009). https://doi.org/10.1144/1470-9236/08-040
62. The Mathworks Inc.: MATLAB—MathWorks, USA (2016)